

Video Article

Light Sheet-based Fluorescence Microscopy of Living or Fixed and Stained *Tribolium castaneum* Embryos

Frederic Strobl^{1,2,3}, Selina Klees^{1,2,3}, Ernst H. K. Stelzer^{1,2,3}

¹Physical Biology, Buchmann Institute for Molecular Life Sciences (BMLS)

²Cluster of Excellence Frankfurt, Macromolecular Complexes

³Goethe-Universität Frankfurt am Main – Campus Riedberg

Correspondence to: Ernst H. K. Stelzer at ernst.stelzer@physikalischebiologie.de

URL: <https://www.jove.com/video/55629>

DOI: [doi:10.3791/55629](https://doi.org/10.3791/55629)

Keywords: Developmental Biology, Issue 122, Arthropod, insect, Coleoptera, *Tribolium castaneum*, morphogenesis, embryogenesis, non-invasive long-term fluorescence live imaging, light sheet-based fluorescence microscopy, three-dimensional light microscopy, LSM, DSLM, SPIM

Date Published: 4/28/2017

Citation: Strobl, F., Klees, S., Stelzer, E.H. Light Sheet-based Fluorescence Microscopy of Living or Fixed and Stained *Tribolium castaneum* Embryos. *J. Vis. Exp.* (122), e55629, doi:10.3791/55629 (2017).

Abstract

The red flour beetle *Tribolium castaneum* has become an important insect model organism in developmental genetics and evolutionary developmental biology. The observation of *Tribolium* embryos with light sheet-based fluorescence microscopy has multiple advantages over conventional widefield and confocal fluorescence microscopy. Due to the unique properties of a light sheet-based microscope, three dimensional images of living specimens can be recorded with high signal-to-noise ratios and significantly reduced photo-bleaching as well as photo-toxicity along multiple directions over periods that last several days. With more than four years of methodological development and a continuous increase of data, the time seems appropriate to establish standard operating procedures for the usage of light sheet technology in the *Tribolium* community as well as in the insect community at large. This protocol describes three mounting techniques suitable for different purposes, presents two novel custom-made transgenic *Tribolium* lines appropriate for long-term live imaging, suggests five fluorescent dyes to label intracellular structures of fixed embryos and provides information on data post-processing for the timely evaluation of the recorded data. Representative results concentrate on long-term live imaging, optical sectioning and the observation of the same embryo along multiple directions. The respective datasets are provided as a downloadable resource. Finally, the protocol discusses quality controls for live imaging assays, current limitations and the applicability of the outlined procedures to other insect species.

This protocol is primarily intended for developmental biologists who seek imaging solutions that outperform standard laboratory equipment. It promotes the continuous attempt to close the gap between the technically orientated laboratories/communities, which develop and refine microscopy methodologically, and the life science laboratories/communities, which require 'plug-and-play' solutions to technical challenges. Furthermore, it supports an axiomatic approach that moves the biological questions into the center of attention.

Video Link

The video component of this article can be found at <https://www.jove.com/video/55629/>

Introduction

The red flour beetle *Tribolium castaneum*, which belongs to the large family of darkling beetles (Tenebrionidae), has a long history within the agricultural and life sciences and is the second best studied model insect model organism after the fruit fly *Drosophila melanogaster*. During the last four decades, it became a powerful and popular insect model organism in developmental genetics, in evolutionary developmental biology and, during the last twenty years, in embryonic morphogenesis for a variety of reasons:

Drosophila and *Tribolium* both belong to the Holometabola, but diverged approximately 300 million years ago^{1,2,3,4}. While the embryonic development of *Drosophila* is commonly considered as highly derived, *Tribolium* shows a more ancestral mode of development that is found in a considerably larger proportion of insect species^{5,6,7,8,9}. Firstly, *Tribolium* exhibits non-involuting head development, i.e. its mouthparts and antennae emerge already during embryogenesis^{10,11,12,13,14,15}. Secondly, *Tribolium* follows the principles of short-germ development, i.e. abdominal segments are added sequentially from a posterior growth zone during germband elongation^{16,17,18,19}. Thirdly, *Tribolium* develops and later degrades two extra-embryonic membranes i.e. the amnion, which covers the embryo only ventrally, and the serosa, which envelops the embryo completely^{20,21,22}. Both membranes play a crucial morphogenetic²³ as well as protective role against microorganisms^{24,25} and desiccation²⁶. Fourthly, the embryonically developing legs are fully functional during the larval life stage and serve as the primordia for the adult legs during pupal metamorphosis^{27,28,29,30,31}.

Due to their small size and modest demands, cultivation of *Tribolium* in the laboratory is fairly straightforward. Cultures of wild-type (WT) strains or transgenic lines typically consist of around 100-300 adults and can be kept within one-liter glass bottles (footprint 80 cm²) filled three to four centimeters high (about 50 g) with growth medium that consists of full grain wheat flour supplemented with inactive dry yeast. A water supply is not necessary. This allows even small laboratories to keep dozens of beetle cultures within small- or medium-sized commercially available

insect incubators. Later developmental stages of *Tribolium* (larvae after approximately the fourth instar, pupae and adults) are easily separated from the growth medium by sieving. Synchronized embryos are obtained by incubating adults for short periods on egg-laying medium. For rapid development, beetle cultures are kept at 32 °C (about four weeks per generation), while stock keeping is typically performed at 22-25 °C (about ten weeks per generation).

Within the last decade, many standard techniques have been gradually adapted and optimized for *Tribolium*, as summarized in the *Emerging Model Organisms* books³². Of great importance are advanced genetic methods such as embryonic³³, larval^{34,35} or parental^{36,37} RNA interference-based gene knockdown, germline transformation with either the *piggyBac*^{38,39} or the *Minos*⁴⁰ transposase system and CRISPR/Cas9-based genome engineering⁴¹. Furthermore, the *Tribolium* genome has been sequenced about a decade ago⁴², and is now in the third round of genome assembly release⁴³, which allows efficient and genome-wide identification and systematic analysis of genes⁴⁴ or other genetic elements^{45,46}. Additionally, the genomes of four other coleopteran species are available for comparative genetic approaches^{47,48,49,50}. In association with the sequenced genome, two large-scale genetic analyses have been performed, *i.e.* an insertional mutagenesis screen⁵¹ and a systematic RNA interference-based gene knockdown screen^{52,53}.

Fluorescence live imaging with widefield, confocal or light sheet-based microscopy (LSFM) allows to observe the embryonic morphology of *Tribolium* as a function of time (*i.e.* the morphogenesis) in a multi-dimensional context (**Table 1**). In widefield and confocal fluorescence microscopy, the excitation and emission light is guided through the same objective lens. In both approaches, the entire specimen is illuminated for every recorded two-dimensional plane. Hence, the specimens are subjected to very high energy levels. In LSFM, only the fluorophores in the focal plane are excited due to a decoupling of illumination and detection by using two perpendicularly arranged objective lenses (**Figure 1**). LSFM comes in two canonic implementations – the single plane illumination microscope (SPIM) and the digital scanned laser light sheet-based fluorescence microscope (DSLM, **Figure 2**) – and offers several crucial advantages over traditional approaches: (i) intrinsic optical sectioning capability, (ii) good axial resolution, (iii) strongly reduced level of photo-bleaching, (iv) very low photo-toxicity, (v) high signal-to-noise ratio, (vi) relatively high acquisition speed, (vii) imaging along multiple directions and (viii) deeper tissue penetration due to the usage of low numerical aperture illumination objective lenses^{54,55,56}.

LSFM has already been successfully applied in *Tribolium* to document nearly the entire embryonic morphogenesis⁵⁷ and to analyze the principles of extra-embryonic membrane rupture at the beginning of dorsal closure²³. To raise the attractiveness of LSFM in the *Tribolium* community and for insect science in general, it is of great importance to establish standard operating procedures and to improve the methods, protocols and the pool of resources to a level where the microscope becomes an ease-of-use standard tool in developmental biology laboratories, and the biological questions stay in the center of attention.

This protocol begins with the basics of *Tribolium* cultivation, *i.e.* maintenance, reproduction and embryo collection. Next, two experimental strategies are illustrated: (i) live imaging of custom-made transgenic lines and (ii) imaging of fixed embryos that were stained with fluorescent dyes (**Table 2**). Subsequently, three mounting techniques with slightly different purposes are explained in detail (**Figure 3** and **Table 3**): (i) the agarose column, (ii) the agarose hemisphere and (iii) the novel cobweb holder. The protocol then explains the data acquisition procedure with LSFM. Imaging modalities and key considerations are outlined. Finally, embryo retrieval is explained and suggestions for basic data processing are provided. In the representative results, live imaging data from two novel custom-made and the Glia-blue⁵⁸ transgenic lines are shown and the respective imaging datasets are provided as a downloadable resource. Additionally, image data of fixed embryos that were stained with a variety of fluorescence dyes are presented. The discussion focuses on quality control, current limitations of the live imaging approach and the adaptation of the protocol to other species.

The protocol is written for light sheet-based fluorescence microscopes that are equipped with a sample chamber and a rotatable clamp mechanism for standardized sample holders^{54,59,60}, which are typically cylinder-shaped elements made of metal, plastic or glass with a diameter in the millimeter range. The protocol is also suitable for both canonic implementations, *i.e.* SPIM and DSLM, as well as for setups with two or more illumination and detection arms^{61,62,63}. The representative results show data in two spectral channels, green (illumination with a 488 nm laser, detection through a 525/50 bandpass filter) and red (illumination with a 561 nm laser, detection through a 607/70 bandpass filter), but the protocol can be expanded to three or four spectral channels.

Protocol

1. Husbandry of *Tribolium* Cultures

NOTE: Standard conditions are defined as an incubation temperature of 25 °C and 70% relative humidity in a 12 h bright/12 h dark cycle. For more information on *Tribolium* husbandry, respective guidelines are available⁶⁴. This protocol requires two different flour-based media, which can be prepared in kilogram quantities and stored for several months.

1. Prior to working with flour and inactive dry yeast, store the unopened packages at -20 °C for 24 h and then let them warm up to room temperature. This procedure eliminates potential pathogens.
2. Pass full grain wheat flour and inactive dry yeast through a sieve with 710 µm mesh size, then prepare growth medium by supplementing the sifted full grain flour with 5% (w/w) sifted inactive dry yeast.
3. Pass 405 fine wheat flour and inactive dry yeast through a sieve with 250 µm mesh size, then prepare egg-laying medium by supplementing the sifted 405 fine wheat flour with 5% (w/w) sifted inactive dry yeast.
4. Pass the respective *Tribolium* culture through a sieve with 800 µm mesh size. Discard the leftover growth medium. Transfer the larvae, pupae and adults to a large glass dish.
5. If no progeny culture exists, transfer around 80 larvae and/or pupae to a new glass bottle to establish a new progeny culture. If no larvae and/or pupae are present, take around 40 adults instead. Add 50 g of growth medium and incubate under standard conditions.
6. Collect around 300 adults (500-700 mg) in another new glass bottle to establish the imaging culture. Add 50 g of growth medium and incubate under standard conditions. Allow the imaging culture to settle for at least 24 h in the fresh growth medium before embryo collection.

7. Replace the growth medium of the imaging culture at least every two weeks, which can be done in conjunction with embryo collection (see 3.2). After two to three months, replace the imaging culture completely by new adults from the progeny culture.
8. If a non-homozygous transgenic line is used, curate the progeny cultures frequently by removing non-transgenic animals. Ideally, generate homozygous lines if the respective transgene is not lethal or causes sterility when present on both chromosomes. Homozygous cultures typically have a higher average fluorescence level and the overall experimental conditions are narrower, since only one genotype is present.

2. Microscope Setup and Calibration

NOTE: The *Tribolium* embryo has an anterior-posterior length of about 600–660 μm and a transversal diameter of about 300–330 μm . Most modern CCD cameras have a sensor chip size of about 9 mm x 7 mm, i.e. a diameter of 11.4 μm , and a pixel-pixel distance of 6.45 μm . When combined with a 10X magnification objective lens, the embryo can be imaged *in toto* with a pixel pitch of 0.645 μm . Most modern sCMOS cameras have a larger sensor chip size of about 16 mm x 14 mm, i.e. a diameter of 21.3 μm , and a pixel-pixel distance of 6.5 μm . When combined with a 20X magnification objective lens, the embryo can be imaged *in toto* with a pixel pitch of 0.325 μm .

1. Attach the illumination and detection objective lenses to the microscope. Ensure that lasers and fluorescence filters match the fluorophore absorption and emission spectra very well.
2. Attach the sample chamber to the microscope. Fill the sample chamber with PBS pH 7.4 or any other appropriate imaging buffer.
3. Switch on and calibrate the microscope. Comprehensive calibration routines and troubleshooting guidelines for custom-built light sheet-based microscopes (more specifically for the DSLM implementation) have been published previously⁶⁵. For commercial devices, follow the manufacturer's instructions very carefully. Mishandling might deplete the sample chamber of the medium and cause havoc to the instrument as well as the specimen.

3. Collection of Transgenic or WT Embryos

1. Pass the imaging colony through a sieve with 800 μm mesh size. Collect adult beetles in a new glass bottle and add 10 g of egg-laying medium. Incubate the egg-laying culture for 1 h at 25 °C and 70% relative humidity in light.
2. Pass the egg-laying culture through a sieve with 800- μm mesh size to separate adults from the egg-laying medium, which contains around 30–100 embryos. Transfer adults to a new glass bottle and add either the old or 50 g of fresh growth medium.
3. If observation should start at the uniform blastoderm stage (example dataset DS0002), incubate the egg-laying medium for 15 h at 25 °C and 70% relative humidity. To start at the beginning of germband retraction (example datasets DS0001 and DS0003), incubate embryos for 23 h at 32 °C and 70% relative humidity. If other developmental stages are desired, refer to the respective literature^{64,65} and adapt incubation time and/or temperature as necessary.

4. Embryo Dechoriation

NOTE: The chorion is the outer layer of the eggshell and consists of proteins and polysaccharides. It is strongly light absorbent but not essential for proper development and can thus be chemically removed.

1. Pass the egg-laying medium through a sieve with 300 μm mesh size. Collect the embryos in a cell strainer with 100 μm mesh size and discard the leftover egg-laying medium.
2. Prepare a 6-well plate as follows: fill the A1, A2, A3 and B3 wells with 10 mL PBS pH 7.4 and the B1 and B2 wells with 9 mL PBS. Then carefully add 1 mL sodium hypochlorite to B1 and B2. Observe the progress of steps 4.3 to 4.8 under the stereo microscope. CAUTION sodium hypochlorite is corrosive.
3. Insert the cell strainer into the A1 well (PBS pH 7.4) and wash the embryos for one minute under gentle agitation. Larger flour particles should detach from the embryos.
4. Transfer the cell strainer to the B1 well (sodium hypochlorite in PBS pH 7.4) and shake the plate vigorously for 30 s. The remaining flour particles should detach completely from the embryos.
5. Transfer the cell strainer to the A2 well (PBS pH 7.4) and wash the embryos for 1 min under gentle agitation.
6. For dechoriation, transfer the cell strainer to the B2 well (sodium hypochlorite in PBS pH 7.4). Shake the plate vigorously until the chorion ruptures and detaches from the embryos. The chorion looks like a thin, semi-transparent membrane with lacerated edges, while dechorionated embryos have a plain silhouette.
7. Transfer the cell strainer to the A3 well (PBS pH 7.4) and wash the embryos for 1 min under gentle agitation. If any chorion fragments are still attached to the embryos after the washing, repeat step 4.6.
8. Store the embryos in the B3 well (PBS pH 7.4). Storage for several hours does not harm the embryos, but keep in mind that development continues.
9. For non-homozygous transgenic lines, remove any non-fluorescent embryos if possible. For fixation and staining of WT or transgenic embryos, continue with step 5. For live imaging of transgenic embryos, continue with step 6.

5. Vitelline Membrane Permeabilization, Fixation, and Staining

NOTE: The vitelline membrane is the inner layer of the eggshell. It is impervious for fluorescent dyes and thus has to be chemically permeabilized before staining.

1. Fill a scintillation vial with fixation/permeabilization solution (1.5 mL 4% (w/v) paraformaldehyde in PBS pH 6.9 and 1.5 mL n-heptane). Transfer embryos with a paintbrush to the vials. Cover vials with aluminum foil to protect fluorophores from light and incubate for 30 min on a rocking platform at 50 rotations per minute. CAUTION paraformaldehyde is toxic and corrosive, n-heptane is flammable and toxic.
2. Remove fixation solution and treat embryos three times for 15 min in 3 mL 0.1% (v/v) Triton X-100 in PBS pH 7.4 and subsequently once for 15 min in 3 mL 1% (v/v) Triton X-100 in PBS pH 7.4 on a rocking platform at 50 rotations per minute. CAUTION Triton X-100 is corrosive.

- Remove permeabilization solution and add 0.5 mL staining solution to the vial. Exemplary staining solutions are provided in **Table 2**. Stain embryos overnight at 4 °C on a rocking platform at 50 rotations per minute. For the dyes proposed in **Table 2**, washing is not necessary.

6. Preparation of Mounting Agarose

- Add 1 g low-melt agarose to 100 mL PBS pH 7.4 and heat the mixture for 2-3 min in a microwave oven at 800 W. If small agarose particles are still present, repeat the heating process in 30 sec intervals until the particles dissolve completely. The mounting agarose does not need to be prepared freshly every time, the solidified agarose can be re-liquefied by heating as described above. This process can be repeated 5-6 times before too much water has evaporated.
- Allow the agarose to cool down to approximately 40-45 °C, then fill two 1.5 mL reaction tubes with the heated agarose and keep those tubes at 35 °C in a thermoblock.

7. Embryo Mounting and Insertion into the Sample Chamber

- Option 1: Agarose column (Figure 3A-C, first column; Table 3, second column)**
 - Fill a 1.0 mL syringe with distilled water and attach it to one of the glass capillary openings by using a small rubber hose. Fill the capillary halfway with distilled water.
 - Pick an embryo with a paintbrush and place it on the inner side of the other glass capillary opening. Proceed quickly to the next step before the embryo dries out.
 - Stick the capillary into the liquid agarose and slowly draw a few μL of liquid agarose alongside the embryo into the capillary. Then quickly increase the drawing force so that the embryo is dragged along with the agarose. In the end, a few μL of agarose should be above and below the embryo. Set the capillary aside for a few minutes and let the agarose solidify.
 - Shorten the capillary with a diamond glass cutter to a length of about 5 mm. The remaining fragment should be completely filled with agarose and the embryo should be within the second quartile.
 - Insert the steel cylinder with the pin into the sample chamber, and then stick the capillary fragment on top of the pin. The agarose column should protrude a few millimeters from the capillary fragment with the part that contains the embryo.
- Option 2: Agarose hemisphere (Figure 3A-C, second column; Table 3, third column)**
 - Draw 200 μL of liquid agarose into a 1.0 mL syringe, then use it to fill the steel pipe from the top with agarose until a hemisphere forms at the bottom opening. The hemisphere diameter should be equal to the pipe diameter. Wait a few minutes until the agarose has solidified.
 - Pick an embryo with a paintbrush and rearrange it on the tip of the brush so that the anterior end becomes accessible. Dip the agarose hemisphere into liquid agarose to cover it with a thin film.
 - Place the embryo with its anterior end upright on the pole of the agarose hemisphere. Turn the steel pipe around and correct the position of the embryo with the brush. If necessary, stabilize the embryo by adding 2 μL agarose to the embryo/hemisphere border. Ideally, less than half of the embryo surface should be covered in agarose and the flanks should be as steep as possible.
 - Insert the steel pipe with the hemisphere and embryo slowly into the sample chamber.
- Option 3: Cobweb holder (Figure 3A-C, third column; Table 3, fourth column)**
 - Pick an embryo with a paintbrush and set it aside.
 - Cover the slotted hole of the cobweb holder with 5-8 μL liquid agarose, then remove most of the agarose until only a thin agarose film remains.
 - Place the embryo onto the agarose film and adjust its position. Carefully move the embryo to the x-axis center of the slotted hole, and align its elongated anterior-posterior axis with the elongated axis of the slotted hole.
 - Insert the cobweb holder with the mounted embryo slowly into the sample chamber. Position the cobweb holder so that it does not interfere with the excitation and emission light, i.e. 45° relative to the x- and z-axis.

8. Light Sheet-based Fluorescence Microscopy

- Decide along how many directions (and along which orientations) the embryo should be imaged. Four directions (along the orientations 0°, 90°, 180° and 270°) typically provide a good trade-off between coverage and energy load.
- Set up the number of fluorescence channels. The major parameters for each channel are the laser line, the fluorescence filter, the laser power and the exposure time. For long-term live imaging, it is important that the integrated energy load does not exceed the tolerance of the embryo. An exposure time of 25-50 ms ensures fast imaging, while a laser power between 100 and 300 μW should not affect the viability of the embryo. For fixed samples, exposure time and laser power can be at least doubled.
- For live imaging assays, configure the time lapse. The complete embryogenesis of *Tribolium* takes about seven days at room temperature (23 ± 1 °C) and a little less than three days at 32-35 °C⁶⁴. Define the temporal interval according to the morphogenetic events that should be observed. For short temporal intervals, consider lowering exposure time and laser power (see 8.2).
- Position the embryo in transmission light mode along the x- and y-axes into the center of the field of view without exposing it to the laser. Rotate the embryo by 360° in 90° steps to examine the embryo for any damage that could have occurred during the mounting process.
- Rotate the embryo appropriately around the y-axis to align the embryonic axes with the microscope axes, for example the lateral axis with the x-axis, i.e. the dorsoventral axis with the z-axis. When using the cobweb holder technique, alignment might not be possible.
- In the fluorescence mode, define the z-stack for each direction. Add 25-50 μm as spatial buffer in front of and behind the embryo. Including the buffer, the typical z-stack covers around 350-400 μm for a *Tribolium* embryo. Also define the z-spacing, which should be four times the lateral spacing, i.e. the spacing along the x- and y-axes⁶⁶.
- If two or more embryos are imaged in parallel, restart at 8.4 with the next embryo.

8. For long-term imaging, ensure that the sample chamber is filled with sufficient PBS pH 7.4 or other imaging buffer. Also cover the sample chamber opening.
9. Start the imaging process. For long-term live imaging, monitor the correct acquisition along all directions in all channels for all embryos. Occasionally check during the next days that the embryos are alive and in the appropriate position.

9. Embryo Retrieval and Quality Control

1. Once imaging has completed, remove the sample holder with the embryos from the sample chamber. Only embryos from live imaging assays have to be retrieved. Fixed and stained embryos can be discarded.
2. If a live imaging assay was performed, transfer the embryo to an object slide. For the agarose column technique, extract the embryos from the surrounding agarose with a scalpel, micro-knife or razor blade. For the agarose hemisphere technique, transfer the hemisphere with the flat side to the object slide. Embryo removal is not necessary. For the cobweb holder technique, gently dismount the embryos from the agarose film with a paintbrush. Incubate the object slide in a small glass dish in saturated humidity atmosphere under standard conditions until the larvae hatch.
3. After hatching, transfer the larvae to individual wells of a 24-well plate and add 500 mg of growth medium to each well. Incubate under standard conditions. Compare the total development time and morphology of the imaged larvae to non-imaged WT and transgenic larvae (see discussion). In assays that characterize WT development, no obvious morphological aberrations should ideally be noticeable.
4. Once the larvae develop to healthy adults, provide them with appropriate WT partners of the same background strain. After two weeks, check for progeny production. Also consider to check the fertility of the progeny by mating them *inter pares*. Only when the imaged embryos develop into fertile adults that produce fertile progeny, the imaging procedure can be considered non-invasive.

10. Image Data Processing

NOTE: For image data processing, the open-source image processing software ImageJ⁶⁷ or its derivate FIJI⁶⁸ are recommended. Both versions as well as comprehensive documentation are found at www.imagej.net. The standard file format for LSM data is the tagged image file format (TIFF). The intrinsic container option allows the storage of image stacks such as z-stacks or time series of z maximum projections within a single file that can be opened in ImageJ or FIJI via drag-and-drop.

1. If necessary, rotate the z-stacks to align the anterior-posterior axis of the embryo with the y-axis (Image → Transform → Rotate). Please note that the rotation parameters have to be set individually for each direction, but not for the time lapse and the fluorescence channels.
2. Crop the z-stacks along the x-, y- and z-axes so that only minimal background (20 - 40 pixels along the x- and y-axes, 5 - 10 planes along the z-axis) remains (for the x- and y-axes, use the Rectangular Selection Tool, then Image → Crop; for the z-axis, use Image → Stacks → Tools → Slice Keeper). Please note that the cropping parameters have to be set individually for each direction, but not for the time points and the fluorescence channels.
3. Calculate the z maximum projection for each z-stack (Image → Stacks → Z Project, choose Max Intensity). Intensity projection calculations are data simplification procedures that remove one spatial dimension.
4. For long-term live imaging data, consider using an ImageJ or FIJI script that performs processing steps 10.1 to 10.3 for all directions, all time points and all fluorescence channels⁶⁵. Ideally, concatenate all z maximum projections per channel and direction and save them as a time series in one TIFF container. Alternatively, the BigDataViewer⁶⁹ plug-in for FIJI can be used to navigate through Terabyte-large datasets.
5. Depending on the transgenic line and imaging modalities, dynamic intensity adjustments of the time stacks might be desirable due to photo-bleaching and/or fluorophore expression fluctuations. Either the ImageJ- or FIJI-intrinsic Bleach Correction function (Image → Adjust → Bleach Correction, choose Histogram Matching) or dedicated software⁶⁵ are suggested.
6. If the embryo was recorded and/or along multiple directions and in multiple fluorescence channels, horizontal combination of the directions (Image → Stacks → Tools → Combine) and channel merge (Image → Color Merge → Channels) are recommended.
7. Registration and fusion of z-stacks acquired along multiple directions⁷⁰, eventually in combination with deconvolution⁷¹, allows the calculation of superior three-dimensional images of uniform quality and isotropic resolution. Both plug-ins are open source and pre-installed in FIJI, but they require the presence of landmarks (fluorescent microspheres, e.g. beads) around the specimen.
8. Open-source software frameworks for large-scale quantitative data extraction and analysis are also available, for example for segmentation and tracking of cell nuclei⁷² or cell shape recognition⁷³.

Representative Results

This protocol describes an experimental framework for fluorescence imaging of living or fixed and stained *Tribolium* embryos with LSM. Due to the low levels of photo-bleaching and photo-toxicity, a direct consequence of its optical sectioning capability, LSM is particularly well suited for long-term live imaging.

The novel AGOC{ATub'H2B-mEmerald} #1 transgenic line expresses a histone2B-mEmerald fusion protein under control of the *alpha-tubulin 1* promoter⁷⁴. It shows an enhancer trap-like expression pattern⁵¹, since the fluorescence signal is mainly obtained from the serosa, the yolk sac and several neuronal cell clusters. Using this line, 66 hr of embryonic development at room temperature (23 ± 1 °C) were recorded, covering germband retraction and dorsal closure (Supplementary Movie 1). This line can be used to visualize neuronal clusters within the head appendages (Figure 4A) and the dynamics of serosa migration during dorsal closure (Figure 4B). The novel AGOC{ATub'H2B-mEmerald} #4 line carries the same transgene as the #1 line, but at a different genomic location. It does not show an obvious enhancer trap pattern, but the fluorescence signal is spatiotemporally ubiquitously detectable as described previously for this promoter⁷⁴. This line was imaged at the transition from gastrulation to germband elongation to demonstrate the optical sectioning capability at two depth levels (Figure 4C). Another feature, especially for live imaging, is the acquisition of z-stacks along multiple directions via sample rotation, which is standard for LSM setups used in developmental biology. For example, in the Glia-blue⁵⁸ line, sample rotation allows the observation of glia cell reorganization along and around the ventral nerve cord as well as the proliferation dynamics in the left head lobe, which can only be seen properly from the dorsal site, in the same embryo (Figure 4D, Supplementary Movie 2). The live imaging datasets associated with this study are provided as a downloadable resource, meta and access information are found in Supplementary Table 1.

Since the choice of transgenic lines for live imaging is still limited, small fluorescent dyes can be used to specifically label intracellular structures. SYTOX Green binds to cell nuclei and can be visualized in the green channel, while YOYO-1 and BOBO-3 iodide bind to the nuclear envelope and can be visualized in the green or red channel, respectively (Figure 5A). These dyes can be used to highlight certain embryonic structures, such as the serosa scar (Figure 5B, first column), the posterior ventral serosa cells (Figure 5B, second column) or the serosa-amnion-germband tissue tri-layer that emerges during serosa window closure (Figure 5B, third to fifth column). Dual-color staining allows the visualization of two intracellular structures in the same embryo, for example the nuclear envelope together with the actin cytoskeleton, which can be stained with Alexa Fluor-conjugated Phalloidin dyes. For example, YOYO-1 iodide can be combined with Phalloidin 546 (Figure 5C), while BOBO-3 can be combined with Phalloidin 488 (Figure 5D).

It is also convenient to fix and stain transgenic embryos that already express a certain fluorescent protein, since the fixation procedure quenches the intrinsic fluorescence signal only marginally. For example, embryos from the AGOC{ATub'H2B-mEmerald} #4 transgenic line, in which the nuclei are detected in the green channel, can be stained with Phalloidin 546 so that the actin cytoskeleton becomes visible in the red channel (Figure 6).

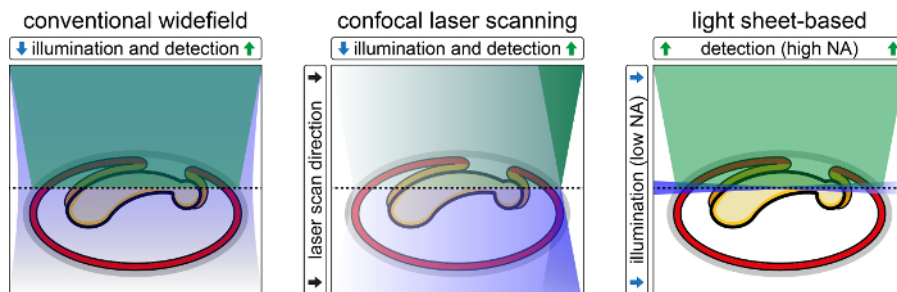


Figure 1: Comparison of Conventional Widefield, Confocal Laser Scanning and Light Sheet-based Fluorescence Microscopy.

Conventional widefield epi-fluorescence microscopy uses xenon arc/mercury-vapor lamps with appropriate filters or high-power light emitting diodes as light sources. For each acquired two-dimensional image, the whole specimen is illuminated with a non-diffraction-limited light cone. In confocal laser scanning fluorescence microscopy, a diffraction-limited Gaussian laser beam is scanned through the specimen and fluorescence is detected incoherently point-by-point. Similarly to conventional widefield epi-fluorescence microscopy, the whole specimen is illuminated for each acquired two-dimensional image. In light sheet-based fluorescence microscopy, a diffraction-limited Gaussian laser beam illuminates the specimen perpendicularly to the detection axis. Fluorescence is detected either plane-by-plane or line-by-line. During the acquisition of a two-dimensional image, only a small volume centered on the focal plane of the detection objective experiences the effects of the excitation light. The remaining volume of the specimen is not illuminated, does not contribute to out-of-focus blur, does not suffer from photo-toxic effects and does not lose fluorophores due to photo-bleaching. [Please click here to view a larger version of this figure.](#)

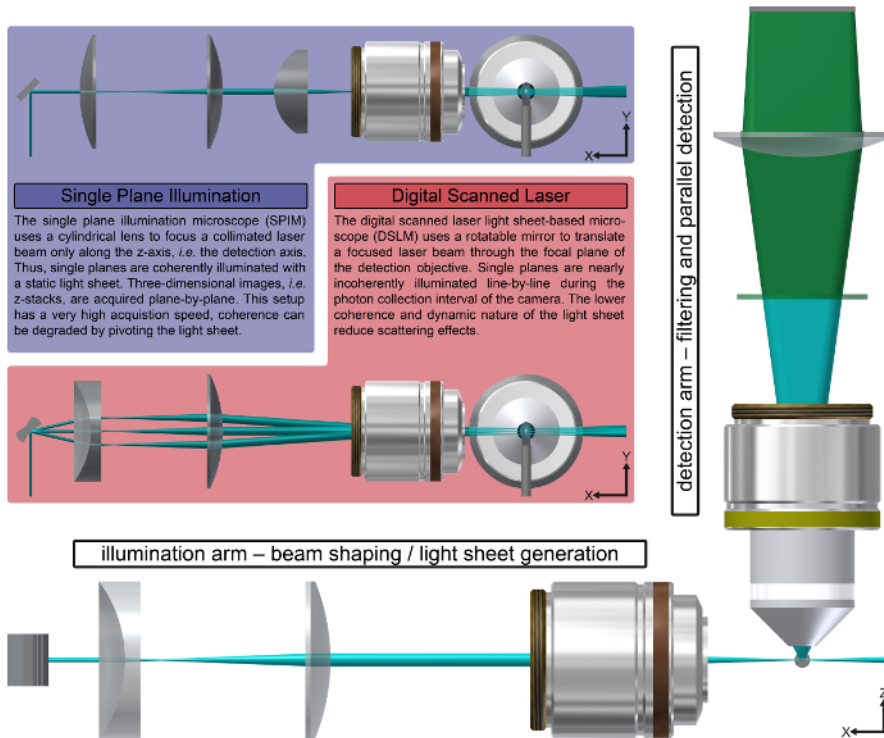


Figure 2: The Principle of Light Sheet-based Fluorescence Microscopy. In LSFM, illumination and detection are split into at least two optical paths. At least one illumination arm is used to generate the light sheet (cyan), while at least one detection arm is equipped with an appropriate filter and a camera for the parallel detection of the fluorescence signal (green). LSFM has two canonic implementations, the single (or selective) plane illumination microscope (blue background) and the digital scanned laser light sheet microscope (red background). By moving the specimen and the light sheet relative to each other, three-dimensional images are acquired. Information along multiple directions is collected by rotating the specimen around the y-axis, which is preferentially oriented along gravity. [Please click here to view a larger version of this figure.](#)

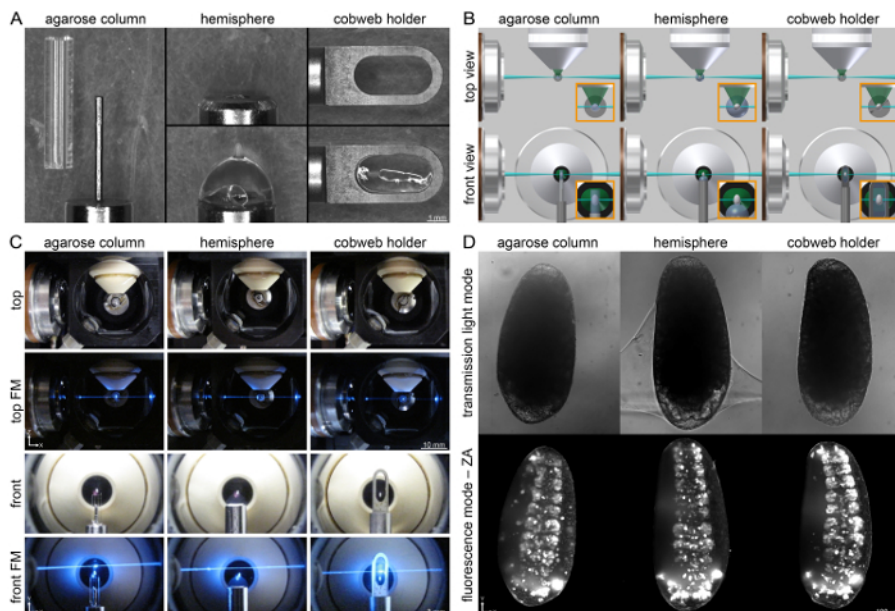


Figure 3: Three Different Mounting Techniques used in the Recording of the Embryonic Development of *Tribolium* with Light Sheet-based Fluorescence Microscopy. (A) The agarose column refers to a steel cylinder with a small pin that pushes the agarose column, in which the embryo is embedded, out of a glass capillary. The agarose hemisphere is mounted on a steel pipe. The embryo is attached to the pole of the hemisphere with a small amount of agarose. The cobweb holder is a sheet of metal with a slotted hole mounted on top of the steel cylinder. The embryo is glued to a thin agarose film that spans the slotted hole. (B) Schemes of the three mounting techniques inside a light sheet microscope. (C) The three mounting techniques applied within a DSLM. (D) Exemplary images from embryos of the Glia-blue transgenic line recorded with the three mounting techniques. The embryos, which are at the onset of germband retraction, are shown with their posterior end orientated towards top to match the transmission light images. FM, fluorescence mode; ZA, z maximum projection with intensity adjustment. [Please click here to view a larger version of this figure.](#)

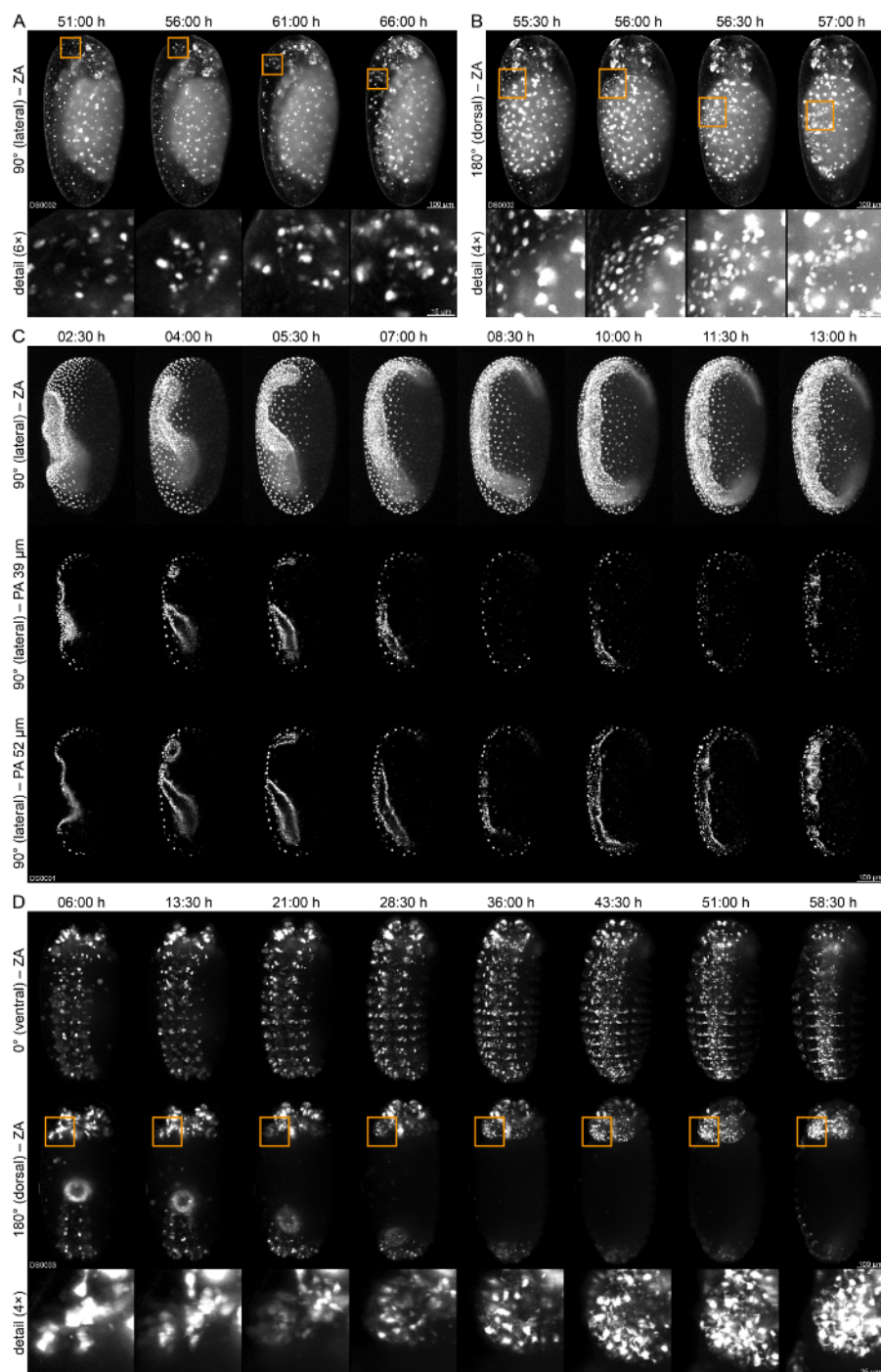


Figure 4: Live Imaging of *Tribolium* Embryos. (A) An embryo of the AGOC{ATub'H2B-mEmerald} #1 line at the transition from germband retraction to dorsal closure. This line exhibits an enhancer trap expression pattern. The fluorescence signal is mainly found in the serosa, the yolk sac and a few neuronal cell clusters. The embryo is shown over a period of 15 h with an interval of 5 h. The detail images show cell clusters in the head appendages. Initially, the clusters are still covered by serosal cells (first column), upon serosa rupture, the cells follow along with the turning movement of the head. (B) Same embryo shown during dorsal closure for 1:30 h with an interval of 0:30 h. The detail images show the migration of the ruptured serosa over the yolk sac. (C) Top row: An embryo of the AGOC{ATub'H2B-mEmerald} #4 line at the transition from gastrulation to germband elongation. Middle and lower row: Single planes are shown in two depths over a period of 10:30 h with an interval of 1:30 h. (D) An embryo of the Glia-blue line during germband retraction shown over a period of 50:30 h with an interval of 07:30 h. The detail images show the morphogenetic reorganization of the glial cells in the left head lobe. ZA, z maximum projection with intensity adjustment; PA single plane with intensity adjustment. [Please click here to view a larger version of this figure.](#)

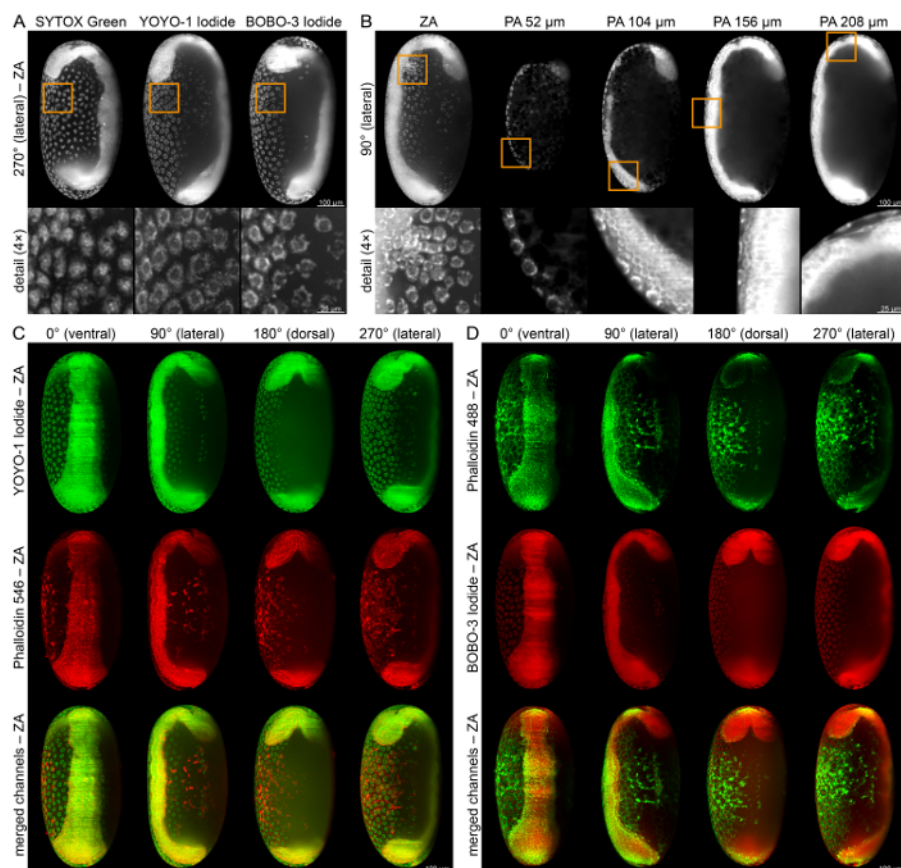


Figure 5: Fixation, Staining, and Imaging of WT Embryos during Germband Elongation. (A) Embryos stained with either SYTOX Green, *i.e.* a fuzzy nuclear stain, or YOYO-1 iodide or BOBO-3 iodide, *i.e.* two nuclear envelope stains. (B) YOYO-1 iodide-stained embryo. Details show the serosa scar (first column), the nuclear envelope of the large posterior-ventral serosa cells (second column) or the three-layered tissue organization of the serosa, the amnion and the actual embryonic tissue (third to fifth column). (C) Dual-color staining with YOYO-1 iodide and Phalloidin 546. (D) Dual-color staining with Phalloidin 488 and BOBO-3 iodide. ZA, z maximum projection with intensity adjustment. [Please click here to view a larger version of this figure.](#)

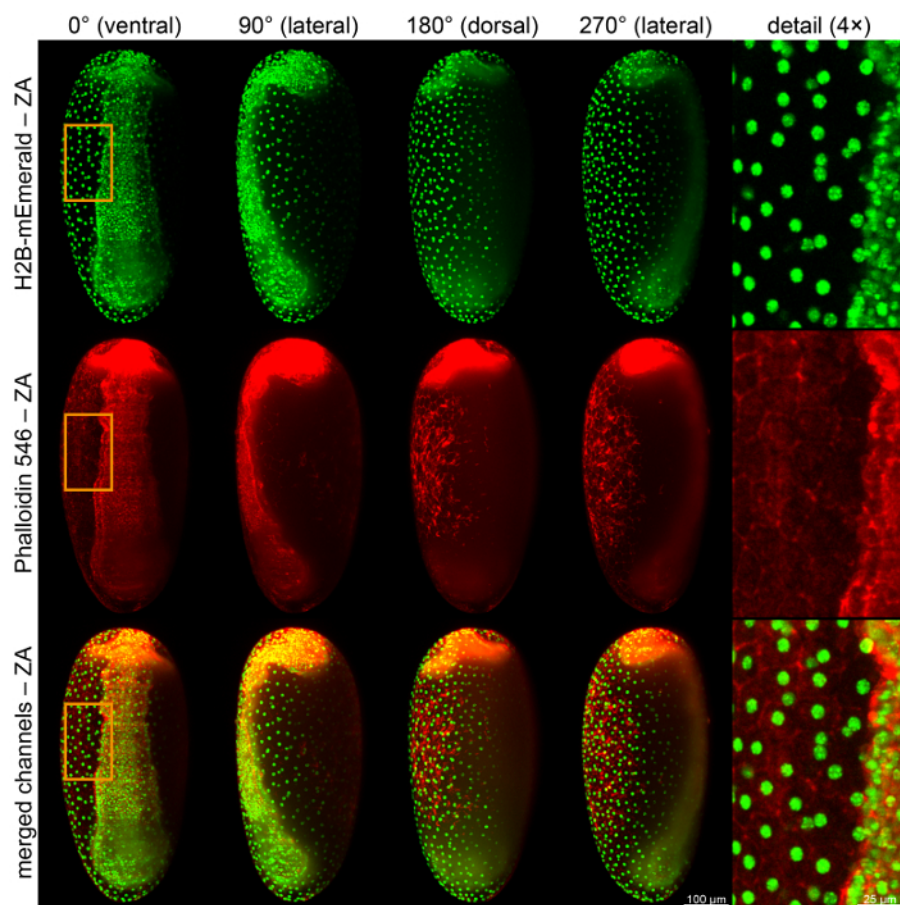


Figure 6: Images of Fixed and Stained Transgenic Embryos from the AGOC{ATub'H2B-mEmerald} #1 line. This transgenic line expresses mEmerald-labeled histone2B (H2B) under control of the *alpha-tubulin 1* promoter, which marks the nuclei/chromatin ubiquitously throughout the whole embryonic development. The embryo was further stained with Alexa Fluor 546 Phalloidin, which labels the actin cytoskeleton/f-actin. ZA, z maximum projection with intensity adjustment. [Please click here to view a larger version of this figure.](#)

criterion	fluorescence microscope type		
	conventional wide field	confocal laser scanning	light sheet-based
objective lens setup	one objective lens, medium-high NA	one objective lens, high NA	two perpendicularly arranged objective lenses, illumination: low NA, detection: high NA
illumination light source	white light source and appropriate filters (e.g. mercury short-arc lamps) or LED-based with clean-up filters	laser with clean-up filter (e.g. diode or DPPS lasers)	laser with clean-up filter (e.g. diode or DPPS lasers)
illumination per two-dimensional image	whole sample	whole sample (typically two-dimensional Gaussian beam scan)	only focal plane (DSLIM: one-dimensional Gaussian beam scan)
detection	parallel (typically CCD or sCMOS camera)	sequential (photomultiplier tube)	parallel (typically CCD or sCMOS camera)
imaging speed	fast (milliseconds per image)	slow (seconds per image)	fast (milliseconds per image)
out-of-focus fluorescence	no discrimination	blocked nearly completely by the pinhole (rejection efficiency depends on diameter)	nearly non-existent (only due to scattering)
spatial dimensions	2 (x / y)	3 (x / y / z)	3 (x / y / z)
further degrees of freedom	2 (time, fluorescence channel)	2 (time, fluorescence channel)	3 (time, fluorescence channel, direction)
lateral resolution	r ($0.6 \lambda / NA$)	$0.66 r$ ($0.4 \lambda / NA$)	r ($0.6 \lambda / NA$)
optical sectioning capability	No	Yes (discrimination in the detection pathway)	Yes (discrimination in the illumination pathway ⁷⁵)
availability and price	predominantly commercial, low cost	predominantly commercial, expensive	commercial, expensive custom-built, moderate ^{54,59,60,75}
live imaging publications covering <i>Tribolium</i> embryos	six ^{44,76,77,78,79,80}	seven ^{23,77,79,81,82,81} (spinning disk confocal) ^{83,84,85}	four ^{23,57,65,86}

Table 1 - Characteristics of Fluorescence Microscopy Techniques used in *Tribolium* live Imaging.

dye	staining	dilution
SYTOX Green	nuclei (fuzzy)	1:10,000 (1:100 in ddH ₂ O and 1:100 in 1% (w/v) BSA in PBS)
YOYO-1 Iodide	nuclear envelope	1:10,000 (1:100 in ddH ₂ O and 1:100 in 1% (w/v) BSA in PBS)
BOBO-3 Iodide	nuclear envelope	1:10,000 (1:100 in ddH ₂ O and 1:100 in 1% (w/v) BSA in PBS)
Alexa Fluor 488 Phalloidin	actin cytoskeleton	1:100 (in 1% (w/v) BSA in PBS)
Alexa Fluor 546 Phalloidin	actin cytoskeleton	1:100 (in 1% (w/v) BSA in PBS)

Table 2 - Staining Solutions.

	agarose column (option 1)	hemisphere (option 2)	cobweb holder (option 3)
rationale	embryo is embedded in an agarose column that is pushed out of a capillary	posterior end of embryo is glued to pole of an agarose hemisphere	embryo is glued to thin agarose film spanning a slotted hole
sample holder	steel cylinder with pin	steel pipe	steel cylinder with slotted hole
directions (orientations)	unlimited (any)	unlimited (any)	four (0°, 90°, 180°, 270°)
required skill level	moderate	high	low
agarose around the embryo	high	low	moderate
number of embryos per session	up to three	one	up to six
embryo retrieval	tricky	easy	easy
disposable equipment	glass capillaries	-	-
recommended for	short-term live imaging, stained embryos	long-term live imaging	long-term live imaging, stained embryos
references	three ^{23,87,88}	two ^{57,65}	this publication

Table 3 - Mounting Methods Advantages and Disadvantages.

aberrational phenotype induction	rationale	step	reference (methodological)
embryonic RNA interference	double-stranded RNA is injected into embryos during the syncytial blastoderm stage to knock-down one or more specific genes	inject embryos after Step 4.8.	two ^{33,81}
parental RNA interference	double-stranded RNA is injected laterally into female pupae between the abdominal segments 3 and 4, which leads to gene knock-down in the progeny	take the pupae from Step 1.5.	two ^{36,37}
recessive embryonic lethal mutant lines	egg-laying cultures that carry a recessive embryonic lethal mutation heterozygous yield about 25% homozygote mutant progeny	cross mutant line into imaging line during Step 1.5.	three ^{39,51,89}
application of extrinsic factors	certain bioactive or toxic factors are extrinsically applied to the embryos by adding them to the imaging buffer	add factor to imaging buffer during Step 2.2.	two ^{83,85}

Table 4 - LSFM Live Imaging of Aberrational Phenotypes

Supplementary Table 1 - Metadata and Parameter for the Long-term Live-imaging Datasets DS0001-0003. [Please click here to download the file.](#)

Supplementary Movie 1 - Live Imaging of a *Tribolium* Embryo from the AGOC{ATub^{H2B-mEmerald}} #1 Transgenic Line.

This line exhibits an enhancer trap expression pattern. The fluorescence signal is primarily found in the serosa, the yolk sac and a subset of neuronal cells. The embryo is shown along four orientations from 00:00 h to 66:00 h with an interval of 00:30 h between the time points. The movie starts at the beginning of germband retraction and ends once dorsal closure is completed. Frame rate is five frames per second. ZA, z maximum projection with intensity adjustment. [Please click here to download the file.](#)

Supplementary Movie 2 - Live Imaging of a *Tribolium* Embryo from the Glia-blue Transgenic Line.

The embryo is shown along four orientations from 00:00 h to 66:00 h with an interval of 00:30 h between the time points. The movie starts at the beginning of germband retraction and ends once dorsal closure is completed. Frame rate is five frames per second. ZA, z maximum projection with intensity adjustment. [Please click here to download the file.](#)

Discussion

Quality control

In live imaging assays, the preparation and recording procedure must be non-invasive, *i.e.* neither the mechanical and chemical handling (collection, dechoriation, mounting onto the sample holder) nor the integrated energy load during the observation should affect the viability of the specimen. For studies that characterize WT development, it is recommended to only use data from experiments in which the embryo

survives the recording process, is retrieved successfully and develops into a healthy adult. The adult should not show any morphological aberrations, should be fertile and its progeny should also be fertile. There are three major reasons for low survival rates, especially in long-term live imaging assays:

Firstly, the embryo surface was covered extensively with agarose during Step 7, which probably hinders ion and gas exchange and constricts the embryo mechanically. Affected embryos, especially when imaged during early embryogenesis, typically develop inconspicuously for several hours, arrest suddenly and lose their fluorescence signal quickly. With some experience, the surface fraction that is embedded in agarose by using the hemisphere technique can be kept below one-third, while with the cobweb holder technique, at most half of the surface is covered by a very thin agarose layer. Secondly, the integrated energy load applied to the embryo exceeds the tolerance. The values given in Step 8.2 serve as a rule of thumb, but the following criteria should be considered: (i) embryos during early embryonic development do not endure laser irradiation as well as embryos during late embryonic development, (ii) although the integrated energy load might be identical, higher laser power with either lower exposure time or longer temporal intervals appears to be more stressful than lower laser power with a high exposure time or shorter temporal intervals, (iii) higher wavelengths are typically better tolerated and (iv) for transgenic lines, the tolerance limit appears to be line-specific, whereas fluorophore expression strength seems to be inversely proportional to the laser irradiation tolerance. Additionally, the design of the fusion protein and/or the intracellular localization also play a role. Thirdly, the embryo is damaged during the mounting process. The most crucial factor here is that the incubation time in the sodium hypochlorite solution is as short as necessary to completely remove the chorion. Longer incubation times might harm the embryos. Care should also be taken to not puncture or squeeze the embryos with the brush and to keep the mounting agarose at an ambient temperature. Damaged embryos can be identified during Step 8.4 before the actual imaging process commences, so that damaged embryos can be replaced with viable ones.

By following those guidelines, typically around 85-90% of the embryos survive the live imaging procedure and hatch. Around 90% of the hatched embryos develop into healthy and fertile adults. The survival ratio appears to be independent from imaging temperature and mounting techniques (when the agarose column is used for imaging periods of not more than half a day), but slightly decreases with elevated levels of laser irradiance. As an additional control, especially during the initial characterization of custom-made transgenic lines for fluorescence live imaging or the framework establishing phase as precursor for a comprehensive experimental sequence, it is recommended to run non-imaged WT and transgenic embryos in parallel to the imaged embryos, which are incubated at the same temperature as the imaged embryo, and compare their development time and morphology⁶⁵.

Furthermore, studies that characterize aberrational phenotypes (**Table 4**) via live imaging should also run a non-affected control embryo in parallel. It is recommended to keep the treatment of both embryos as similar as possible, but this has to be considered individually for each experimental strategy:

Knock-down via RNA interference.

For embryonic RNA interference^{33,81}, embryos that derive from the same egg-laying culture should either be injected with functional or control double-stranded RNA. The differently injected embryos should then be imaged simultaneously in the same LSMF by using either the agarose column or the cobweb holder technique. For parental RNA interference^{36,37}, the imaging culture should be split into two subcultures. Female pupae of one subculture should be injected with the functional double-stranded RNA, while the other subculture should be injected with control double-stranded RNA. Embryo collection should be performed in parallel, and both the experimental and the control embryo can be imaged simultaneously in the same microscope by using the agarose column or cobweb holder technique.

Recessive embryonic lethal mutant lines.

When working with recessive embryonic lethal mutants^{39,89,91,92,93}, an egg-laying culture of heterozygous mutants, which are normally phenotypically inconspicuous, yields theoretically 25% homozygous mutant progeny (but sometimes less due to practical handling issues⁸⁹) and 75% of phenotypically inconspicuous progeny (50% heterozygous mutants and 25% WTs). It is recommended to use the cobweb holder technique to mount several embryos from such an egg-laying culture. The homozygous mutants can be identified throughout the course of imaging by the manifestation of the phenotype, while the normally developing embryos serve as controls. The genotype of the imaged specimens can be determined once imaging and quality control are completed.

Application of extrinsic factors.

If the influence of extrinsic factors within the imaging buffer^{83,85}, e.g. bioactive or toxic substances, on development is investigated, parallel imaging together with a control embryo in the same LSMF is typically not possible. Therefore, imaging has to be performed sequentially. Optimally, the time between subsequent experiments is minimized and the embryos derive from the same imaging culture. Alternatively, two identically constructed and operated LSMFs can be used. In this case, embryos from the same egg-laying period should be used, but it is of great importance that the calibration of both microscope is conducted carefully so that the imaging properties are comparable. By using the cobweb holder technique, multiple embryos for each condition can be imaged at once. With the agarose column technique, the extrinsic factors might be hindered from reaching the embryos.

Current limitations of the LSMF live imaging approach

LSMF is a powerful tool to analyze embryonic morphogenesis non-invasively in multiple broad-scaled dimensions. Standard operation procedures, as proposed in this protocol, will support the process to establish light sheet technology as a standard tool in developmental biology. However, the approach is limited by a number of factors on diverse experimental and organizational levels:

Initially, LSMF was developed to analyze one specimen at a time. All current approaches that image two or more embryos simultaneously in the same microscope by 'stacking' the specimen along the y-axis in the agarose column or the cobweb holder addresses this issue only to a certain degree. Multi-well plate- and coverslip-based setups are available^{94,95,96}. However, they suffer from reduced image quality and sacrifice some of the essential benefits from LSMF, such as imaging along multiple directions. Currently, the best option is to work with multiple microscopes in parallel, which becomes reasonably feasible when costly components, such as the laser, are shared⁶⁰.

With the EFA-nGFP^{57,65,84}, the FNL⁸⁶, the Brainy^{58,86}, the AGOC{ATub'H2B-mEmerald} #1, the AGOC{ATub'H2B-mEmerald} #4 and the Glia-blue⁵⁸, only six custom-made transgenic lines suitable for long-term live imaging are currently available. In addition, the HC079 (amnion), G12424 (serosa) and G04609 (heart) enhancer trap lines⁵¹ have been characterized with LSF²³. Alternatively, fluorescent embryos can also be generated by mRNA⁹¹ or dye injection⁷⁹, those approaches are relatively straightforward, but also suffer from limitations⁸⁶. Several more standards are still required such as cytoskeletal-, organelle- and membrane-labeled lines or lines that express fluorophores under certain non-ubiquitous promoters to observe only certain organs or tissues. Ideally, those lines are also available with different fluorescent proteins.

Another challenge is the data volume generated by LSF. Due to acquisition of information in three spatial dimensions and at least three further degrees of freedom (time, direction, fluorescence channel), the size of live imaging datasets can easily reach many Gigabytes to a few Terabytes. Even after three-dimensional cropping and ZIP-based compression of the TIFF containers, the three exemplary datasets associated with this study have sizes of 31.6, 12.6 and 45.1 Gigabytes, i.e. 89.3 Gigabyte in total. When working with LSF, it is necessary to have the respective infrastructure for data storage and processing^{88,97}.

The highest image quality is obtained at the surface of the embryo, but with increasing depth, the fluorescence signal becomes more and more blurry. For example, the posterior end of the germband becomes covered by the yolk sac fold during gastrulation and cannot be properly resolved (Figure 4C, first to fifth column). Imaging along multiple directions solves this problem at least partially – high quality information from the surface all around the embryo is available, but the inner regions remain fuzzy. Currently, no satisfying solutions are available, but in the long run, infrared fluorescent proteins⁹⁸, genetic approaches⁹⁹ or microscope setups with adaptive optics¹⁰⁰ could be considered.

Adaptation for other species

By now, LSF has been used to document the embryonic development of three insect species, i.e. the fruit fly *Drosophila melanogaster*^{61,62,101}, the scuttle fly *Megaselia abdita*¹⁰² and the red flour beetle *Tribolium castaneum*⁵⁷. The experimental framework, standard operating procedures and mounting techniques described here should be easily adaptable to other insect species. Germline transformation protocols for many insects that belong to various orders are available¹⁰³, including species of economical and/or medical importance, such as the honeybee¹⁰⁴, several lepidopterans^{105,106} or multiple mosquito species^{107,108,109}. With respective transgenic lines suitable for fluorescence live imaging, the embryonic morphogenesis of insects can be characterized while considering their evolutionary lineages and/or ecological niches. About one million insect species have been described and a further twenty million insect species most likely exist¹¹⁰, covering more than 400 million years of evolution². Only the comparative approach will generate information that in turn provides insights which cannot be obtained by studying the developmental principles of only a single species.

Disclosures

The authors have nothing to disclose.

Author Contributions

FS and EHKS conceived the research. FS generated the transgenic AGOC lines. Light sheet-based fluorescence imaging was performed by FS and SK. FS and EHKS wrote the manuscript with input from SK.

Acknowledgements

We thank Sven Plath for technical support. The Glia-blue transgenic line was a kind gift from Gregor Bucher (Göttingen, Germany). The research was funded by the Cluster of Excellence Frankfurt am Main for Macromolecular Complexes (CEF-MC, EXC 115, speaker Volker Dötsch) granted in part to EHKS at the Buchmann Institute for Molecular Life Sciences (BMLS, director Enrico Schleiff) at the Goethe Universität Frankfurt am Main by the Deutsche Forschungsgemeinschaft (DFG).

References

1. Brown, S. J., Denell, R. E., & Beeman, R. W. Beetling around the genome. *Genet. Res.* **82**, 155-61 (2003).
2. Misof, B. *et al.* Phylogenomics resolves the timing and pattern of insect evolution. *Science*. **346**, 763-7 (2014).
3. Tong, K. J., Duchêne, S., Ho, S. Y. W., & Lo, N. INSECT PHYLOGENOMICS. Comment on "Phylogenomics resolves the timing and pattern of insect evolution". *Science*. **349**, 487 (2015).
4. Kjer, K. M. *et al.* INSECT PHYLOGENOMICS. Response to Comment on "Phylogenomics resolves the timing and pattern of insect evolution". *Science*. **349**, 487 (2015).
5. Klingler, M. *Tribolium*. *Curr. Biol.* **14**, R639-40 (2004).
6. Savard, J., Marques-Souza, H., Aranda, M., & Tautz, D. A segmentation gene in *tribolium* produces a polycistronic mRNA that codes for multiple conserved peptides. *Cell*. **126**, 559-69 (2006).
7. Yang, X., Zarinkamar, N., Bao, R., & Friedrich, M. Probing the *Drosophila* retinal determination gene network in *Tribolium* (I): The early retinal genes *dachshund*, *eyes absent* and *sine oculis*. *Dev. Biol.* **333**, 202-14 (2009).
8. Peel, A. D. Forward genetics in *Tribolium castaneum*: opening new avenues of research in arthropod biology. *J. Biol.* **8**, 106 (2009).
9. Lynch, J. A., El-Sherif, E., & Brown, S. J. Comparisons of the embryonic development of *Drosophila*, *Nasonia*, and *Tribolium*. *Wiley Interdiscip. Rev. Dev. Biol.* **1**, 16-39 (2012).
10. Schröder, R., Jay, D. G., & Tautz, D. Elimination of EVE protein by CALI in the short germ band insect *Tribolium* suggests a conserved pair-rule function for even skipped. *Mech. Dev.* **80**, 191-195 (1999).
11. Posnien, N., Schinko, J. B., Kittelmann, S., & Bucher, G. Genetics, development and composition of the insect head--a beetle's view. *Arthropod Struct. Dev.* **39**, 399-410 (2010).

12. Posnien, N., Koniszewski, N. D. B., Hein, H. J., & Bucher, G. Candidate gene screen in the red flour beetle *Tribolium* reveals six3 as ancient regulator of anterior median head and central complex development. *PLoS Genet.* **7**, e1002416 (2011).
13. Angelini, D. R., Smith, F. W., Aspiras, A. C., Kikuchi, M., & Jockusch, E. L. Patterning of the adult mandibulate mouthparts in the red flour beetle, *Tribolium castaneum*. *Genetics.* **190**, 639-54 (2012).
14. Coulcher, J. F., & Telford, M. J. Cap'n'collar differentiates the mandible from the maxilla in the beetle *Tribolium castaneum*. *Evodevo.* **3**, 25 (2012).
15. Peel, A. D. *et al.* Tc-knirps plays different roles in the specification of antennal and mandibular parasegment boundaries and is regulated by a pair-rule gene in the beetle *Tribolium castaneum*. *BMC Dev. Biol.* **13**, 25 (2013).
16. Bucher, G., & Klingler, M. Divergent segmentation mechanism in the short germ insect *Tribolium* revealed by giant expression and function. *Development.* **131**, 1729-40 (2004).
17. Handel, K., Basal, A., Fan, X., & Roth, S. *Tribolium castaneum* twist: gastrulation and mesoderm formation in a short-germ beetle. *Dev. Genes Evol.* **215**, 13-31 (2005).
18. Roth, S., & Hartenstein, V. Development of *Tribolium castaneum*. *Development Genes and Evolution.* **218**, 115-118 (2008).
19. Schröder, R., Beermann, A., Wittkopp, N., & Lutz, R. From development to biodiversity--*Tribolium castaneum*, an insect model organism for short germband development. *Dev. Genes Evol.* **218**, 119-26 (2008).
20. Sharma, R., Beermann, A., & Schröder, R. The dynamic expression of extraembryonic marker genes in the beetle *Tribolium castaneum* reveals the complexity of serosa and amnion formation in a short germ insect. *Gene Expr. Patterns.* **13**, 362-71 (2013).
21. Benton, M. A., & Pavlopoulos, A. *Tribolium* embryo morphogenesis: may the force be with you. *Bioarchitecture.* **4**, 16-21 (2014).
22. Horn, T., Hilbrant, M., & Panfilio, K. A. Evolution of epithelial morphogenesis: phenotypic integration across multiple levels of biological organization. *Front. Genet.* **6**, 303 (2015).
23. Hilbrant, M., Horn, T., Koelzer, S., & Panfilio, K. A. The beetle amnion and serosa functionally interact as apposed epithelia. *Elife.* **5**, (2016).
24. Jacobs, C. G. C. C., & van der Zee, M. Immune competence in insect eggs depends on the extraembryonic serosa. *Dev. Comp. Immunol.* **41**, 263-9 (2013).
25. Jacobs, C. G. C., Spaink, H. P., & van der Zee, M. The extraembryonic serosa is a frontier epithelium providing the insect egg with a full-range innate immune response. *Elife.* **3**, (2014).
26. Jacobs, C. G. C., Rezende, G. L., Lamers, G. E. M., & van der Zee, M. The extraembryonic serosa protects the insect egg against desiccation. *Proc. Biol. Sci.* **280**, 20131082 (2013).
27. Lewis, D. L., DeCamillis, M., & Bennett, R. L. Distinct roles of the homeotic genes *Ubx* and *abd-A* in beetle embryonic abdominal appendage development. *Proc. Natl. Acad. Sci. U. S. A.* **97**, 4504-9 (2000).
28. Beermann, A. *et al.* The Short antennae gene of *Tribolium* is required for limb development and encodes the orthologue of the *Drosophila* Distal-less protein. *Development.* **128**, 287-97 (2001).
29. Grossmann, D., Scholten, J., & Prpic, N.-M. Separable functions of wingless in distal and ventral patterning of the *Tribolium* leg. *Dev. Genes Evol.* **219**, 469-79 (2009).
30. Angelini, D. R., Smith, F. W., & Jockusch, E. L. Extent With Modification: Leg Patterning in the Beetle *Tribolium castaneum* and the Evolution of Serial Homologs. *G3 (Bethesda).* **2**, 235-48 (2012).
31. Grossmann, D., & Prpic, N.-M. Egrf signaling regulates distal as well as medial fate in the embryonic leg of *Tribolium castaneum*. *Dev. Biol.* **370**, 264-272 (2012).
32. *Emerging Model Organisms: A Laboratory Manual, Volume 2.* Cold Spring Harbour Laboratory Press. (2010).
33. Brown, S. J., Mahaffey, J. P., Lorenzen, M. D., Denell, R. E., & Mahaffey, J. W. Using RNAi to investigate orthologous homeotic gene function during development of distantly related insects. *Evol. Dev.* **1**, 11-5 (1999).
34. Tomoyasu, Y., & Denell, R. E. Larval RNAi in *Tribolium* (Coleoptera) for analyzing adult development. *Dev. Genes Evol.* **214**, 575-8 (2004).
35. Linz, D. M., Clark-Hachtel, C. M., Borràs-Castells, F., & Tomoyasu, Y. Larval RNA interference in the red flour beetle, *Tribolium castaneum*. *J. Vis. Exp.* e52059 (2014).
36. Bucher, G., Scholten, J., & Klingler, M. Parental RNAi in *Tribolium* (Coleoptera). *Curr. Biol.* **12**, R85-6 (2002).
37. Posnien, N. *et al.* RNAi in the red flour beetle (*Tribolium*). *Cold Spring Harb. Protoc.* **2009**, pdb.prot5256 (2009).
38. Lorenzen, M. D. *et al.* piggyBac-mediated germline transformation in the beetle *Tribolium castaneum*. *Insect Mol. Biol.* **12**, 433-40 (2003).
39. Berghammer, A. J., Weber, M., Trauner, J., & Klingler, M. Red flour beetle (*Tribolium*) germline transformation and insertional mutagenesis. *Cold Spring Harb. Protoc.* **2009**, pdb.prot5259 (2009).
40. Pavlopoulos, A., Berghammer, A. J., Averof, M., & Klingler, M. Efficient transformation of the beetle *Tribolium castaneum* using the Minos transposable element: quantitative and qualitative analysis of genomic integration events. *Genetics.* **167**, 737-46 (2004).
41. Gilles, A. F., Schinko, J. B., & Averof, M. Efficient CRISPR-mediated gene targeting and transgene replacement in the beetle *Tribolium castaneum*. *Development.* **142**, 2832-9 (2015).
42. Richards, S. *et al.* The genome of the model beetle and pest *Tribolium castaneum*. *Nature.* **452**, 949-55 (2008).
43. Kim, H. S. *et al.* BeetleBase in 2010: revisions to provide comprehensive genomic information for *Tribolium castaneum*. *Nucleic Acids Res.* **38**, D437-42 (2010).
44. Stappert, D., Frey, N., von Levetzow, C., & Roth, S. Genome-wide identification of *Tribolium* dorsoventral patterning genes. *Development.* **143**, 2443-54 (2016).
45. Pavlek, M., Gelfand, Y., Plohl, M., & Meštrović, N. Genome-wide analysis of tandem repeats in *Tribolium castaneum* genome reveals abundant and highly dynamic tandem repeat families with satellite DNA features in euchromatic chromosomal arms. *DNA Res.* **22**, 387-401 (2015).
46. Vlahović, I., Glunčić, M., Rosandić, M., Ugarković, Đ., & Paar, V. Regular higher order repeat structures in beetle *Tribolium castaneum* genome. *Genome Biol. Evol.* (2016).
47. Keeling, C. I. *et al.* Draft genome of the mountain pine beetle, *Dendroctonus ponderosae* Hopkins, a major forest pest. *Genome Biol.* **14**, R27 (2013).
48. Vega, F. E. *et al.* Draft genome of the most devastating insect pest of coffee worldwide: the coffee berry borer, *Hypothenemus hampei*. *Sci. Rep.* **5**, 12525 (2015).
49. Cunningham, C. B. *et al.* The Genome and Methyloome of a Beetle with Complex Social Behavior, *Nicrophorus vespilloides* (Coleoptera: Silphidae). *Genome Biol. Evol.* **7**, 3383-96 (2015).
50. Meyer, J. M. *et al.* Draft Genome of the Scarab Beetle *Oryctes borbonicus* on La Réunion Island. *Genome Biol. Evol.* **8**, 2093-105 (2016).

51. Trauner, J. *et al.* Large-scale insertional mutagenesis of a coleopteran stored grain pest, the red flour beetle *Tribolium castaneum*, identifies embryonic lethal mutations and enhancer traps. *BMC Biol.* **7**, 73 (2009).
52. Schmitt-Engel, C. *et al.* The iBeetle large-scale RNAi screen reveals gene functions for insect development and physiology. *Nat. Commun.* **6**, 7822 (2015).
53. Dönitz, J. *et al.* iBeetle-Base: a database for RNAi phenotypes in the red flour beetle *Tribolium castaneum*. *Nucleic Acids Res.* **43**, D720-5 (2015).
54. Keller, P. J., & Stelzer, E. H. K. Digital scanned laser light sheet fluorescence microscopy. *Cold Spring Harb. Protoc.* **2010**, pdb.top78 (2010).
55. Weber, M., & Huiskens, J. Light sheet microscopy for real-time developmental biology. *Curr. Opin. Genet. Dev.* **21**, 566-72 (2011).
56. Stelzer, E. H. K. Light-sheet fluorescence microscopy for quantitative biology. *Nat. Methods.* **12**, 23-6 (2015).
57. Strobl, F., & Stelzer, E. H. K. Non-invasive long-term fluorescence live imaging of *Tribolium castaneum* embryos. *Development.* 1-8 (2014).
58. Koniszewski, N. D. B. *et al.* The insect central complex as model for heterochronic brain development-background, concepts, and tools. *Dev. Genes Evol.* (2016).
59. Gualda, E. J. *et al.* OpenSpinMicroscopy: an open-source integrated microscopy platform. *Nat. Methods.* **10**, 599-600 (2013).
60. Pitrone, P. G. *et al.* OpenSPIM: an open-access light-sheet microscopy platform. *Nat. Methods.* **10**, 598-9 (2013).
61. Tomer, R., Khairy, K., Amat, F., & Keller, P. J. Quantitative high-speed imaging of entire developing embryos with simultaneous multiview light-sheet microscopy. *Nat. Methods.* **9**, 755-63 (2012).
62. Krzic, U., Gunther, S., Saunders, T. E., Streichan, S. J., & Hufnagel, L. Multiview light-sheet microscope for rapid in toto imaging. *Nat. Methods.* **9**, 730-3 (2012).
63. Chhetri, R. K. *et al.* Whole-animal functional and developmental imaging with isotropic spatial resolution. *Nat. Methods.* **12**, 1171-8 (2015).
64. Brown, S. J. *et al.* The red flour beetle, *Tribolium castaneum* (Coleoptera): a model for studies of development and pest biology. *Cold Spring Harb. Protoc.* **2009**, pdb.emo126 (2009).
65. Strobl, F., Schmitz, A., & Stelzer, E. H. K. Live imaging of *Tribolium castaneum* embryonic development using light-sheet-based fluorescence microscopy. *Nat. Protoc.* **10**, 1486-1507 (2015).
66. Engelbrecht, C. J., & Stelzer, E. H. Resolution enhancement in a light-sheet-based microscope (SPIM). *Opt. Lett.* **31**, 1477-9 (2006).
67. Schneider, C. A., Rasband, W. S., & Eliceiri, K. W. NIH Image to ImageJ: 25 years of image analysis. *Nat. Methods.* **9**, 671-675 (2012).
68. Schindelin, J. *et al.* Fiji: an open-source platform for biological-image analysis. *Nat. Methods.* **9**, 676-82 (2012).
69. Pietzsch, T., Saalfeld, S., Preibisch, S., & Tomancak, P. BigDataViewer: visualization and processing for large image data sets. *Nat. Methods.* **12**, 481-483 (2015).
70. Preibisch, S., Saalfeld, S., Schindelin, J., & Tomancak, P. Software for bead-based registration of selective plane illumination microscopy data. *Nat. Methods.* **7**, 418-9 (2010).
71. Preibisch, S. *et al.* Efficient Bayesian-based multiview deconvolution. *Nat. Methods.* **11**, 645-8 (2014).
72. Amat, F. *et al.* Fast, accurate reconstruction of cell lineages from large-scale fluorescence microscopy data. *Nat. Methods.* **11**, 951-8 (2014).
73. Stegmaier, J. *et al.* Real-Time Three-Dimensional Cell Segmentation in Large-Scale Microscopy Data of Developing Embryos. *Dev. Cell.* **36**, 225-240 (2016).
74. Siebert, K. S., Lorenzen, M. D., Brown, S. J., Park, Y., & Beeman, R. W. Tubulin superfamily genes in *Tribolium castaneum* and the use of a Tubulin promoter to drive transgene expression. *Insect Biochem. Mol. Biol.* **38**, 749-755 (2008).
75. Greger, K., Swoger, J., & Stelzer, E. H. K. Basic building units and properties of a fluorescence single plane illumination microscope. *Rev. Sci. Instrum.* **78**, 23705 (2007).
76. El-Sherif, E., Averof, M., & Brown, S. J. A segmentation clock operating in blastoderm and germband stages of *Tribolium* development. *Development.* (2012).
77. Panfilio, K. a, Oberhofer, G., & Roth, S. High plasticity in epithelial morphogenesis during insect dorsal closure. *Biol. Open.* **2**, 1108-18 (2013).
78. Koelzer, S., Kölsch, Y., & Panfilio, K. A. Visualizing late insect embryogenesis: extraembryonic and mesodermal enhancer trap expression in the beetle *Tribolium castaneum*. *PLoS One.* **9**, e103967 (2014).
79. Nakamoto, A. *et al.* Changing cell behaviours during beetle embryogenesis correlates with slowing of segmentation. *Nat. Commun.* **6**, 6635 (2015).
80. Horn, T., & Panfilio, K. A. Novel functions for Dorsocross in epithelial morphogenesis in the beetle *Tribolium castaneum*. *Development.* **143**, 3002-11 (2016).
81. Benton, M. A., Akam, M., & Pavlopoulos, A. Cell and tissue dynamics during *Tribolium* embryogenesis revealed by versatile fluorescence labeling approaches. *Development.* **140**, 3210-20 (2013).
82. van der Zee, M. *et al.* Innexin7a forms junctions that stabilize the basal membrane during cellularization of the blastoderm in *Tribolium castaneum*. *Development.* **142**, 2173-83 (2015).
83. Macaya, C. C., Saavedra, P. E., Cepeda, R. E., Nuñez, V. A., & Sarrazin, A. F. A *Tribolium castaneum* whole-embryo culture protocol for studying the molecular mechanisms and morphogenetic movements involved in insect development. *Dev. Genes Evol.* **226**, 53-61 (2016).
84. Sarrazin, A. F., Peel, A. D., & Averof, M. A Segmentation Clock with Two-Segment Periodicity in Insects. *Science.* **336**, 338-341 (2012).
85. Nollmann, F. I. *et al.* A photorhabdus natural product inhibits insect juvenile hormone epoxide hydrolase. *Chembiochem.* **16**, 766-71 (2015).
86. Strobl, F., & Stelzer, E. H. Long-term fluorescence live imaging of *Tribolium castaneum* embryos: principles, resources, scientific challenges and the comparative approach. *Curr. Opin. Insect Sci.* **18**, 17-26 (2016).
87. Keller, P. J., Schmidt, A. D., Wittbrodt, J., & Stelzer, E. H. K. Digital scanned laser light-sheet fluorescence microscopy (DSLIM) of zebrafish and *Drosophila* embryonic development. *Cold Spring Harb. Protoc.* **2011**, 1235-43 (2011).
88. Reynaud, E. G., Peychl, J., Huiskens, J., & Tomancak, P. Guide to light-sheet microscopy for adventurous biologists. *Nat. Methods.* **12**, 30-4 (2015).
89. Cerny, A. C., Bucher, G., Schröder, R., & Klingler, M. Breakdown of abdominal patterning in the *Tribolium* Krüppel mutant jaws. *Development.* **132**, (2005).
90. Keller, P. J., Schmidt, A. D., Wittbrodt, J., & Stelzer, E. H. K. Reconstruction of zebrafish early embryonic development by scanned light sheet microscopy. *Science.* **322**, 1065-9 (2008).
91. Sulston, I. A., & Anderson, K. V. Embryonic patterning mutants of *Tribolium castaneum*. *Development.* **122**, (1996).
92. Berghammer, A., Bucher, G., Madersbacher, F., & Klingler, M. A system to efficiently maintain embryonic lethal mutations in the flour beetle *Tribolium castaneum*. *Dev. Genes Evol.* **209**, 382-389 (1999).

93. Brown, S. *et al.* Implications of the *Tribolium* Deformed mutant phenotype for the evolution of Hox gene function. *Proc. Natl. Acad. Sci. U. S. A.* **97**, 4510 (2000).
94. Wu, Y. *et al.* Inverted selective plane illumination microscopy (iSPIM) enables coupled cell identity lineaging and neurodevelopmental imaging in *Caenorhabditis elegans*. *Proc. Natl. Acad. Sci.* **108**, 17708-17713 (2011).
95. Kumar, A. *et al.* Dual-view plane illumination microscopy for rapid and spatially isotropic imaging. *Nat. Protoc.* **9**, 2555 (2014).
96. McGorty, R. *et al.* Open-top selective plane illumination microscope for conventionally mounted specimens. *Opt. Express.* **23**, 16142-53 (2015).
97. Amat, F. *et al.* Efficient processing and analysis of large-scale light-sheet microscopy data. *Nat. Protoc.* **10**, 1679-96 (2015).
98. Shcherbakova, D. M., & Verkhusha, V. V. Near-infrared fluorescent proteins for multicolor in vivo imaging. *Nat. Methods.* **10**, 751-4 (2013).
99. Supatto, W., McMahon, A., Fraser, S. E., & Stathopoulos, A. Quantitative imaging of collective cell migration during *Drosophila* gastrulation: multiphoton microscopy and computational analysis. *Nat. Protoc.* **4**, 1397-1412 (2009).
100. Royer, L. A. *et al.* Adaptive light-sheet microscopy for long-term, high-resolution imaging in living organisms. *Nat. Biotechnol.* (2016).
101. Keller, P. J. *et al.* Fast, high-contrast imaging of animal development with scanned light sheet-based structured-illumination microscopy. *Nat. Methods.* **7**, 637-42 (2010).
102. Caroti, F., Urbansky, S., Wosch, M., & Lemke, S. Germ line transformation and in vivo labeling of nuclei in Diptera: report on *Megaselia abdita* (Phoridae) and *Chironomus riparius* (Chironomidae). *Dev. Genes Evol.* **225**, 179-186 (2015).
103. Handler, A. M. Use of the piggyBac transposon for germ-line transformation of insects. *Insect Biochem. Mol. Biol.* **32**, 1211-1220 (2002).
104. Schulte, C., Theilenberg, E., Müller-Borg, M., Gempe, T., & Beye, M. Highly efficient integration and expression of piggyBac-derived cassettes in the honeybee (*Apis mellifera*). *Proc. Natl. Acad. Sci. U. S. A.* **111**, 9003-8 (2014).
105. Tamura, T. *et al.* Germline transformation of the silkworm *Bombyx mori* L. using a piggyBac transposon-derived vector. *Nat. Biotechnol.* **18**, 81-4 (2000).
106. Marcus, J. M., Ramos, D. M., & Monteiro, A. Germline transformation of the butterfly *Bicyclus anynana*. *Proc. R. Soc. B Biol. Sci.* **271**, S263-S265 (2004).
107. Catteruccia, F. *et al.* Stable germline transformation of the malaria mosquito *Anopheles stephensi*. *Nature.* **405**, 959-62 (2000).
108. Grossman, G. L. *et al.* Germline transformation of the malaria vector, *Anopheles gambiae*, with the piggyBac transposable element. *Insect Mol. Biol.* **10**, 597-604 (2001).
109. Labbé, G. M. C., Nimmo, D. D., & Alphey, L. piggybac- and PhiC31-mediated genetic transformation of the Asian tiger mosquito, *Aedes albopictus* (Skuse). *PLoS Negl. Trop. Dis.* **4**, e788 (2010).
110. Patel, N. H. It's a bug's life. *Proc. Natl. Acad. Sci. U. S. A.* **97**, 4442-4 (2000).